CONF-900466--61

MECHANICAL PROPERTIES OF COATINGS AND INTERFACES

B.D. FABES* AND W.C. OLIVER**
*University of Arizona, Department of Materials Science and Engineering, Tucson, AZ 85712
**Oak Ridge National Laboratories, Metals and Ceramics Division, Oak Ridge, TN 37831

CONF-900466--61

DE90 012726

ABSTRACT

Silica Coatings of various thicknesses, hardnesses, and interface integrities were deposited on sapphire substrates using sol-gel techniques. The mechanical properties of the coatings were examined using a mechanical properties microprobe. The observed changes in hardness with indentation depth are explained on the basis of a model of the indentation sequence, in which three separate stages of the indentation process are described. In the first stage, the properties of the coating alone are probed; in the second stage, as the plastic field associated with the indenter extends beyond the coating into the substrate, the properties of the substrate begin to appear; and in the third stage, where the indenter penetrates into the substrate, the composite hardness is dominated by that of the substrate, although the properties of the coating are still apparent.

I. INTRODUCTION

Recent advances in instrumentation have enabled the mechanical properties of exceptionally small volumes (<1 nm) of materials to be probed in a routine fashion [1]. One of the most natural uses of this kind of instrumentation (such as the Nanoindenter*) is the characterization thin coatings and films. Since the net hardness of a composite coating/substrate system is a complicated function of the thickness of the coating, the hardness of the coating, the hardness of the substrate, and the adhesion between the coating and substrate, most previous work using standard indentation techniques has failed to differentiate the effects of all of these parameters. Using the Nanoindenter, however, it should be possible to observe and quantify the effects of these parameters. The goal of this research is to understand the affects coating thickness, hardness, substrate hardness, and interfacial adhesion on the mechanical properties of a composite coating/substrate system.

Here we report on initial progress in developing a refined model of composite hardness. We show, first, that an existing model based on a volume law of mixing is unable to account for the observed variation of hardness with indent depth in a variety of silica coatings on sapphire substrates. Building upon the existing volume law of mixing approaches, we present a qualitative model where the composite hardness is broken down into three stages of the indentation process. Each stage is dependent in some way on the hardness of the coating, the hardness of the substrate, the thickness of the coating, and the adhesion between the coating and substrate.

II. EXPERIMENTAL PROCEDURES

Six sol-gel derived silica coatings were dip-coated on c-cut sapphire substrates. The coating solutions were prepared by acid catalyzed hydrolysis (pH = 2) of tetraethoxysilane (TEOS) using 2 moles of TEOS per mole of H_2O [See 2 for details]. After aging the solutions for at least two weeks, dip coatings were made by withdrawing the substrates from the solution.

To provide an intentionally weakened interface, three of the substrates were covered with 130 Å of sputter deposited gold before dip coating. To examine the effects of coating thickness, the samples were withdrawn from the

* Nanoindenter, manufactured by Nano Instruments Inc., Knoxville, TN USA.

---

coating solution using a variable rate of withdraw, which resulted in a linear gradient in the thickness of the coating. Before firing, the thickness of each coating varied from approximately 300 nm at the thick end to about 100 nm at the thin end. Finally, the samples were fired in air to 100 °C, 400 °C, and 800 °C, one sample with a weakened (Au-coated) interface, and one sample with an unperturbed interface at each temperature.

Indentation experiments were performed using the Nanoindenter with a loading rate of 1 nm/s for the top 30 nm of each sample, and then at 2 nm/s until the maximum load was achieved. The elastic response during indentation was determined by adding a small AC current source to the loading coil. The in-phase displacements were then detected using a lock-in amplifier and the hardness was determined from load/displacement curves using the lock-in data as described elsewhere [3,4]. To account for any irregularities in the shape of the diamond, a polished silica block was indented and used as a standard. The hardness of the silica was assumed to be 14 GPa throughout, and a correction factor was generated for each indentation depth to account for any deviation from this value. This correction was then applied at each depth for each indentation experiment. To determine the indentation size effect (ISE) of the substrate, an uncoated sapphire substrate was also tested. The results presented here are the average of eight indentation experiments for each sample.

III. RESULTS

The measured hardness versus indent depth curves for the 100 °C, sapphire interface coatings are shown in Figure 1a. The curves are typical for sol-gel derived silica coatings on a hard substrate [5]. Near the surface there is a hard "crust," with enhanced hardness. Further into the coating, the hardness appears relatively insensitive to the indent depth until, at larger depths, the properties of the sapphire substrate are apparent, and the hardness increases rapidly. For thicker coatings, the depth at which the properties of the substrate become apparent increases. Upon heating (Figures 1b and c) the hardness of the coatings increases, and the depth at which the properties of the substrate becomes apparent decreases.

The hardnesses of the Au coated sapphire substrates are shown in Figures 2a-c. Again, the hardness increases with firing temperature and the depth at which the properties of the substrate becomes apparent decreases. For all of the Au coated samples, however, the length of the depth-independent region is larger than the corresponding non-Au coated samples, and the hardness drops noticeably, especially for the fired samples, near the sol-gel/Au interface.

IV. DISCUSSION

To quantify the effects of coating hardness, thickness, and interface characteristics on the composite hardnesses observed in Figures 1 and 2, it is helpful to consider the plastic interaction volumes associated with the indents. Burnett and Rickerby suggested that the interaction volume of a hardness indent can be estimated using an expanding spherical cavity model [6]. Using Sargent's idea that the net (composite) hardness of a thin coating should be a weighted average of the plastically deformed volume in the film (V_f) and that in the substrate (V_s)[7], they came up with an equation of the form

$$H_c = \frac{V_f}{V} H_f + \frac{V_c}{V} (\chi^3) H_c \qquad (1),$$

where V is the total volume of plastically deformed material ($V = V_s + V_f$), d is the depth of the indenter, and $H_f = H_f(d)$ and $H_s = H_s(d)$, due to the indentation size effect (ISE). χ is an empirically determined parameter which describes the ability of the plastic zone to extend from the coating

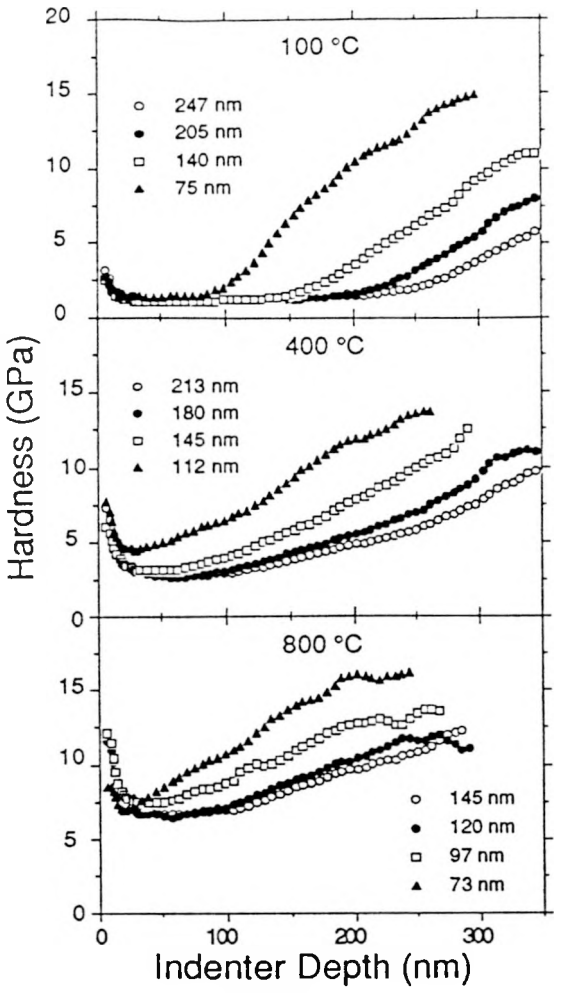

Figure 1: Hardness of TEOS coatings on sapphire. Different symbols refer to different coating thicknesses.

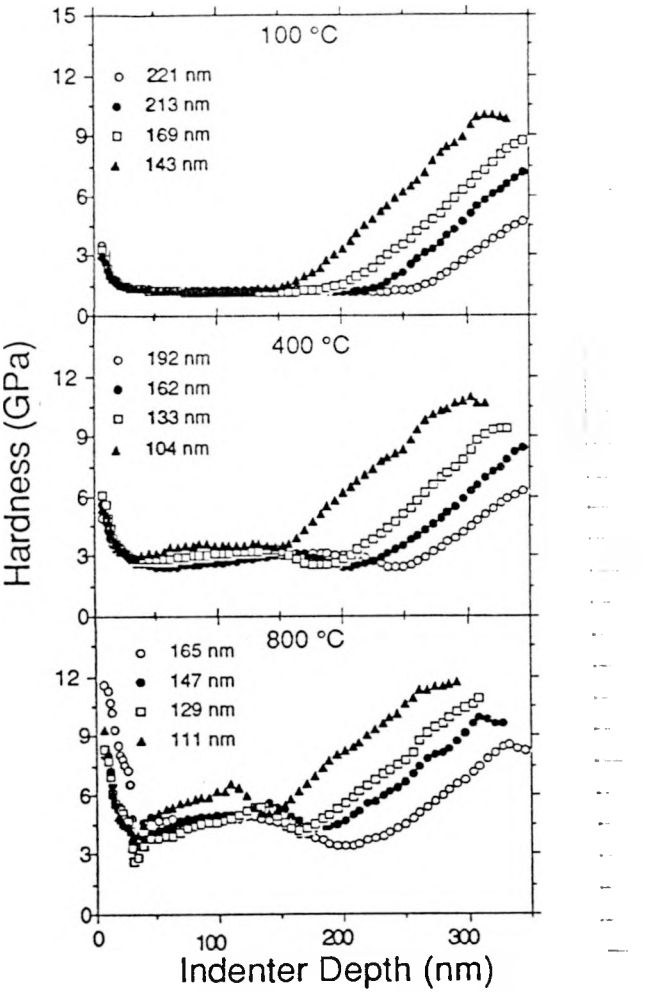

Figure 2: Hardness of TEOS coatings on Au-coated sapphire. Different symbols refer to different coating thicknesses.

into the substrate. This parameter is controlled by the relative hardnesses of the film and substrate, as determined by the mismatch in plastic zone sizes. According to the expanding spherical cavity model [8], the mismatch in plastic zone sizes is given by the ratio $(E_f/H_f)/(E_s/H_s)$, where E_f is the elastic modulus of the film and E_s is the elastic modulus of the substrate. As shown in Figure 3a, for relatively soft films, the plastic zone is restricted more to the coating, while for harder films, the zone is able to protrude further into the substrate. χ is also affected by the integrity of the coating/substrate interface, as an interface which is unable to transmit the shear stresses from the coating to the substrate (Figure 3a), reduces χ, while a well adhering interface allows the stresses to be transmitted more effectively (Figure 3b) to the substrate.

By measuring the composite hardness and the ISE of the substrate, Burnett and Rickerby were able to fit data from a variety of coating/substrate systems to Equation (1), using the ISE of the coating and χ as independent parameters [9,10]. The coarseness of their data allowed a fit to be made without having to consider extremely shallow indents, where the indenter may be wholly supported by the coating or the transition from this stage to where the indenter penetrates into the substrate. The sensitivity of the Nanoindenter, however, should allow these effects to be observed, so Burnett and Rickerby's model must be expanded.

Building on the idea that the interaction volume can be estimated using an expanding spherical cavity model, we postulate that the data in Figures 1 and 2 can be explained on the basis of three stages of the indentation

process. These stages are drawn in Figure 4 for the present case of a softer coating on a harder substrate In the first stage, the plastic zone of the indenter is restricted to the coating, and has not reached the coating/substrate interface. In the second stage, the plastic zone extends into the substrate, while the indenter is still in the coating alone. Finally, in the third region, the indenter has penetrated into the substrate. Below we make some qualitative estimates of the effects of the coating hardness, thickness, and interface integrity on the composite hardness in each of these regions.

Stage I: Plastic Zone Confined to Coating

In the first stage of the indentation process (Figure 4a) neither the indenter nor its associated plastic strain field has reached the coating/substrate interface. The extent of the plastic strain field (b) in the expanding cavity model is given by

$$b = ac\left(\frac{E}{H}\right)^{1/2} \qquad (2)$$

where E is the elastic modulus of the coating material, H is its hardness, c is a geometrical constant, and a is a characteristic linear dimension of the indent, such as the half-diagonal or edge length [8]. Thus, this first stage should extend until the plastic zone size, equals t, the coating thickness. In the nanoindentation experiments the linear dimension is proportional to the square root of the contact area, so that the first stage extends until some depth, d, where

$$b = ac\left(\frac{E}{H}\right)^{1/2} = k\sqrt{area} = t \qquad (3)$$

Equation (3) indicates that the extent of the first stage should be constant (K = 1/k) on a plot of hardness versus $\sqrt{area}/t$. As shown in Figure 5, K has a value of approximately 1.5-2 for the unfired sol-gel coatings. As the hardness and modulus of the coatings change with firing, the extent of the plastic zone changes by a factor of $(E/H)^{1/2}$. Hence, K also changes, to about 0.15 for the coating fired to 400 °C, and to roughly 0.25 for the coatings fired to 800 and 1000 °C.

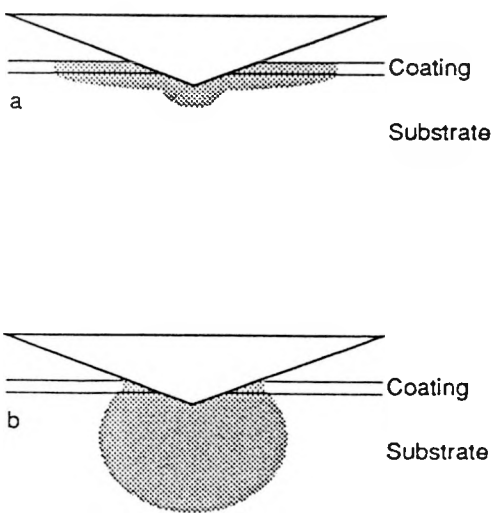

Figure 3: Shape of plastic zones (shaded region) for (a) soft coating on hard substrate and (b) hard coating on soft substrate. After [6].

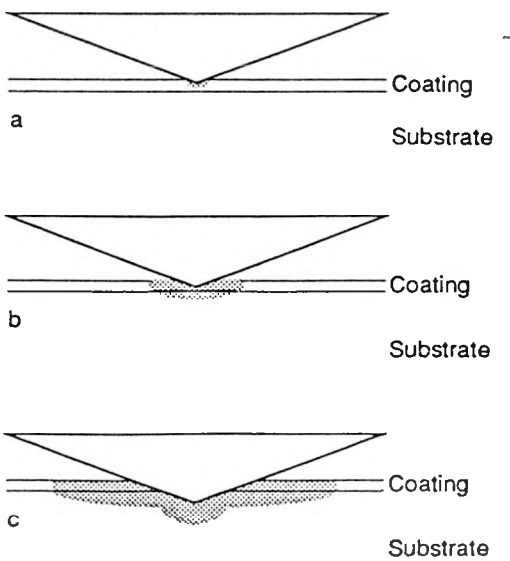

Figure 4: Extents of plastic zones for a softer coating on a harder substrate. (a) Region I: plastic zone is confined to the coating; (b) Region II: plastic zone extends into the substrate; (c) Region III: indenter penetrates substrate.

Also according to Equation (3), the extent of the first stage of the indentation process should be independet of the integrity of the coating/substrate bond. This is demonstrated in Figure 6 where we see that the extent of the first stage is rougly the same for two coatings of the same thicknesses, one on an Au coated substrate and one on a clean substrate.

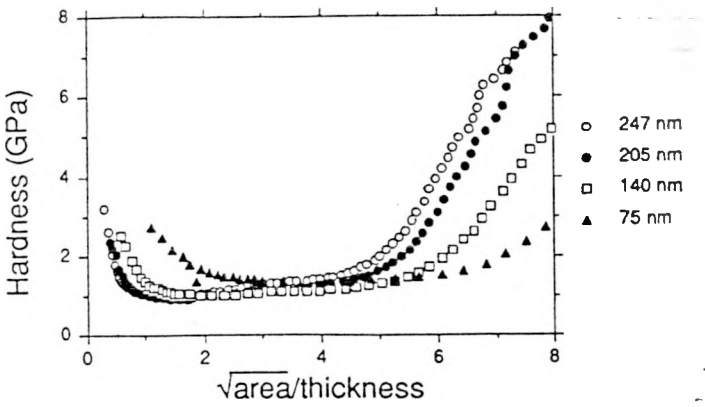

Figure 5: Hardness vs. normalized depth for TEOS coatings on sapphire, fired to 100 °C

Stage II: Interaction of the Plastic Zone with the Substrate

In the second stage of the indentation process (Figure 4b) the plastic zone has exceeded the thickness of the coating, and may now interact with the substrate. As shown in Figures 1a and b and discussed by Burnett and Rickerby, the extent of the protrusion of the plastic zone into the substrate will depend both on the ratio of the hardnesses of the coating and the substrate, as well as on the integrity of the interface. Because higher coating hardnesses and stronger bonding both act to increase the hardness, and because firing the sol-gel coatings increases both the hardness and interfacial bonding, it is difficult to separate these affects. It is possible to make qualitative assertions, however. For example, the transfer of the plastic strains across the interface should improve as the hardness of the coating approaches that of the substrate. This is shown in Figure 7 for three coatings on clean sapphire fired to 100, 400, and 800 °C. As the hardness of the coatings increases, the rate of rise of the hardness in the second region increases.

The integrity of the interface should also affect the hardness. For example, weaker interfaces should inhibit the transfer of the plastic strains across the interface. This is shown in Figure 6, for two coatings with the same hardness and thickness, one on a clean sapphire substrate and one on an Au-coated substrate. The hardness of the coating on the Au coated substrate is independent of depth for the entire region, while there is a noticeable increase in the hardness of the sample on the clean substrate.

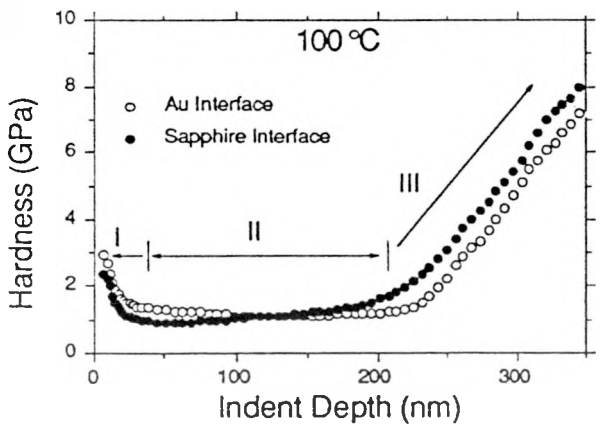

Figure 6: Hardness vs. indent depth for 205 nm TEOS coatings on sapphire and on Au-coated sapphire.

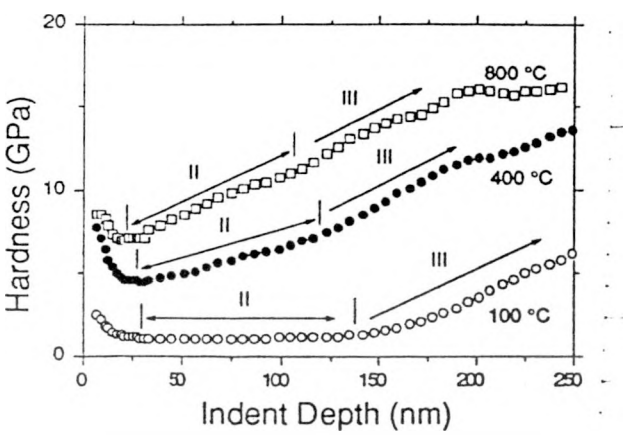

Figure 7: Hardness vs. indent depth for TEOS coatings on sapphire substrates.

Stage III: Penetration of the Indenter Into the Substrate

Once the indenter penetrates the substrate, a sharp rise in the hardness is observed. For all samples this depth correlates well the thickness of the coating. The hardness in this region depends mostly on the relative values of the coating hardness and that of the substrate. The integrity of the interface has little effect of the hardness in this region, since the substrate is deformed directly by the indenter: the plastic zone does not need to be transfered across the interface. This is shown in Figure 6, where the slopes of the hardnesses of the Au and sapphire interfaces are nearly identical in the third region. Only the curvature at the start of the third region is affected, albeit slightly, by the interface. The weaker interface shows a slightly sharper upturn, since the effects of the substrate are masked until the indenter actually enters the substrate.

The thickness of the coating has a nominal affect on the hardness in the third region. Thicker coatings support a slightly larger fraction of the total deformation volume, so that the slope of the hardness curve increases slightly for thinner coatings (Figures 1 and 2). However, the changes are minimal.

V. SUMMARY

We have shown that nanometer sized indents can be used to probe the structure of thin films, with sufficiently high resolution that effects of the coating thickness, coating hardness, and interfacial bonding can be observed. We have also proposed a qualitative model that describes the interactions in three regions of the indentation process. To make the model quantitative, it will be necessary to conduct experiments with systems where the coating hardness and interfacial bonding can be varied independently, and where the hardness of the coating is constant with depth.

VI. REFERENCES

1. W.C. Oliver, R. Hutchings, and J.B. Pethica, in Microindentation Techniques in Materials Science and Engineering, ASTM STP 889, P.J. Blau and B.R. Lawn, eds, pp. 90-108
2. B.D. Fabes and D.R. Uhlmann, *J. Am. Ceram. Soc.*, in press.
3. J.B.Pethica and W.C. Oliver, *Mat. Res. Soc. Symp. Proc.*, 130 (1989) 13.
4. M.F. Doerner, and W.D. Nix, *J. Mater. Res.* 1 (1986) p.601.
5. B.D. Fabes and W.C. Oliver, *J. Non-Cryst. Sol.*, in press.
6. P.J. Burnett and D.S. Rickerby, *Thin Solid Films*, 148 (1987) 41.
7. P.M. Sargent in Microindentation Techniques in Materials Science and Engineering, ASTM STP 889, P.J. Blau and B.R. Lawn, eds, pp. 160-174.
8. B.R. Lawn, A.G. Evans, and D.B. Marshall, *J. Am. Ceram. Soc.*, 63 (1980) 574.
9. P.J. Burnett and D.S. Rickerby, *Thin Solid Films* 148 (1987) 51.
10. P.J. Burnett and T.F. Page, *J. Mat. Sci.*, 19 (1984) 845.

VII. ACKNOWLEDGEMENTS

This research was sponsored in part by the Division of Materials Science, U.S. Department of Energy, under contract DE-AC05-840R2100 with Martin Marietta Energy Systems, Inc., and through the SHaRE Program, under contract DE-AC05-760R00033 with Oak Ridge Associated Universities.